Published online 3 August 2016

Nucleic Acids Research, 2016, Vol. 44, No. 18 ***8885–8896***
doi: 10.1093/nar/gkw689

Force and twist dependence of RepC nicking activity on torsionally-constrained DNA molecules

Cesar L. Pastrana[1,†], Carolina Carrasco[1,†], Parvez Akhtar[2], Sanford H. Leuba[3], Saleem A. Khan[2] and Fernando Moreno-Herrero[1,*]

[1]Department of Macromolecular Structures, Centro Nacional de Biotecnología, CSIC, Darwin 3, 28049 Cantoblanco, Madrid, Spain, [2]Department of Microbiology and Molecular Genetics, University of Pittsburgh School of Medicine, 450 Technology Drive, Pittsburgh, PA 15219, USA and [3]Department of Cell Biology, University of Pittsburgh School of Medicine, Pittsburgh, PA 15213, USA

Received May 18, 2016; Revised July 21, 2016; Accepted July 22, 2016

ABSTRACT

Many bacterial plasmids replicate by an asymmetric rolling-circle mechanism that requires sequence-specific recognition for initiation, nicking of one of the template DNA strands and unwinding of the duplex prior to subsequent leading strand DNA synthesis. Nicking is performed by a replication-initiation protein (Rep) that directly binds to the plasmid double-stranded origin and remains covalently bound to its substrate 5′-end via a phosphotyrosine linkage. It has been proposed that the inverted DNA sequences at the nick site form a cruciform structure that facilitates DNA cleavage. However, the role of Rep proteins in the formation of this cruciform and the implication for its nicking and religation functions is unclear. Here, we have used magnetic tweezers to directly measure the DNA nicking and religation activities of RepC, the replication initiator protein of plasmid pT181, in plasmid sized and torsionally-constrained linear DNA molecules. Nicking by RepC occurred only in negatively supercoiled DNA and was force- and twist-dependent. Comparison with a type IB topoisomerase in similar experiments highlighted a relatively inefficient religation activity of RepC. Based on the structural modeling of RepC and on our experimental evidence, we propose a model where RepC nicking activity is passive and dependent upon the supercoiling degree of the DNA substrate.

INTRODUCTION

Plasmids play a crucial role in prokaryotic evolution by transferring DNA between bacterial species. Although plasmids replicate autonomously, they coexist stably within the host and maintain their copy number by duplicating the DNA before every cell division. There are three main replication mechanisms for circular plasmids: theta-type, strand displacement and rolling-circle (1). Rolling-Circle Replication (RCR) is the most common mode of replication for small (<10 kbp), promiscuous, multi-copy plasmids in Gram-positive bacteria that often carry antibiotic resistance genes (2,3). RCR plasmids of Gram-positive bacteria have been minimally subdivided into four families, pT181, pE194, pSN2 and pC194/pUB110, on the basis of primary sequence homology between initiator proteins and leading-strand origins (4). RCR is initiated by replication initiator proteins (Rep proteins) encoded by the plasmid. The origins of replication of the plasmid contain the binding sites of the Rep proteins as well as their nicking sites (5). Rep proteins are able to nick and ligate DNA through a type I topoisomerase mechanism (3,6).

RepC is a 38-kDa homodimeric protein encoded by the pT181 plasmid of *Staphylococcus aureus*. It binds to a specific DNA sequence contained within the double-stranded origin of replication (*dso*) of the plasmid and creates a nick (Figure 1, step I) (7,8). The nicking site is contained within an inverted repeat that is likely to form a cruciform structure (9). RepC nicks the leading strand and becomes covalently bound to its 5′-end via a phosphotyrosine linkage. Then, PcrA helicase loads onto the short length of accessible single-stranded DNA (ssDNA) (9,10) (Figure 1, step II). The free 3′-end at the nick is used for extension synthesis where PcrA, DNA polymerase III and single-strand DNA binding protein (SSB) coordinate their activities at the origin to replicate the entire plasmid (Figure 1, step III) (11). Replication of DNA by DNA polymerase III proceeds until the plasmid is fully unwound and a new leading strand has been fully synthesized. During elongation, the displaced leading strand forms a single-stranded loop that is protected by SSB proteins from nuclease degradation (12). SSB protein also greatly stimulates the incorporation

*To whom correspondence should be addressed. Tel: +34 91 585 5305; Fax: +34 91 585 4506; Email: Fernando.Moreno@cnb.csic.es
†These authors contributed equally to this work as the first authors.

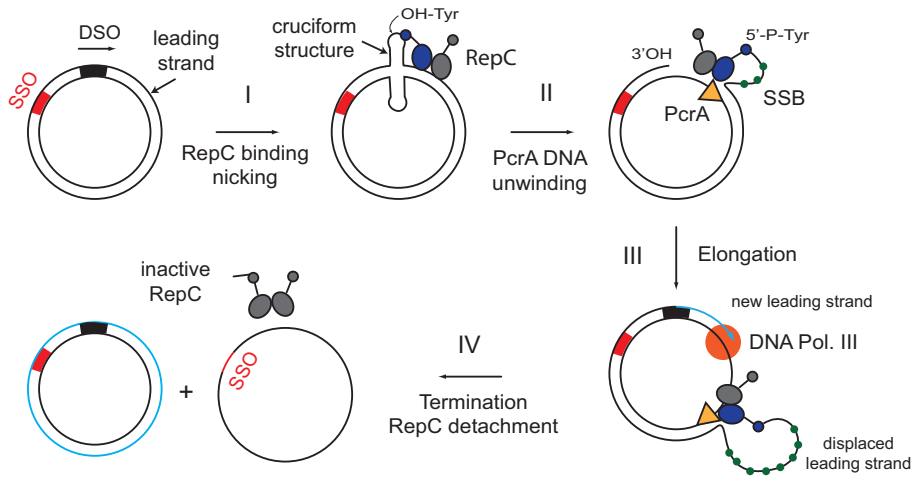

Figure 1. General mechanism of plasmid rolling-circle replication (RCR). (**Step I**) A supercoiled plasmid containing the double-strand origin (*dso*) and single-strand origin (*sso*) is the substrate for DNA replication and is first nicked by a RepC dimer. A secondary structure at the *dso* facilitates binding and/or nicking of the DNA by RepC which becomes covalently attached to the 5′-P end of the DNA after nicking. (**Step II**) PcrA helicase interacts with RepC and unwinds the duplex DNA displacing the leading strand of the plasmid and leaving a free 3′-OH end at the *dso*. (**Step III**) DNA polymerase III loads at the free 3′end and synthesize a new leading strand. The displaced leading strand is protected by SSB proteins. (**Step IV**) A covalently closed single-stranded DNA is produced that can be subsequently converted to dsDNA which involves the synthesis of an RNA primer at the *sso* by the RNA polymerase followed by DNA synthesis by DNA polymerases I and III.

of nucleotides *in vitro* by blocking non-productive binding of the DNA polymerase to ssDNA (13). At the termination step, the other monomer of RepC protein cleaves the displaced ssDNA at the regenerated nick site at the junction of the old and newly synthesized leading strands (14). Next, in a process that is not fully understood, the nick is sealed by RepC leaving a relaxed, closed circular double-stranded DNA (dsDNA) containing the newly synthesized leading strand (Figure 1, step IV). The relaxed DNA is supercoiled (SC) by DNA gyrase while the RepC protein is released from the DNA in an inactive form, covalently bound to a short DNA fragment (15). The displaced single leading strand is then converted to the double-stranded form by using the single strand origin (*sso*) of replication, and requires RNA polymerase for primer synthesis and DNA polymerases I and III for replication (2,16,17).

Formation of a cruciform structure at the *dso* has long been proposed, as it contains multiple inverted repeats at this region (Supplementary Figure S1) (9,18). However, the role of this potential secondary structure of DNA for RepC binding and/or activity is still unclear. Rep proteins have been proposed to induce the formation of a cruciform structure at the *dso* binding site (8,9,19). This model of cruciform formation could be considered as active in that the binding of the protein melts the DNA and actively extrudes the cruciform structure. We instead propose here that RepC plays a passive role in this process and that cleavage only occurs when particular conditions of force and twist on the DNA are fulfilled.

To quantitatively investigate the roles of DNA force and twist in RCR, we have used Magnetic Tweezers (MT) to directly measure the nicking activity of RepC in several kilo basepair long DNA molecules with different degrees of supercoiling and at different applied forces. RepC exclusively nicked negatively supercoiled DNAs and this activity was force-dependent. We have also used MT to measure the relaxation velocity of supercoiled DNA upon nicking and compared RepC data with that obtained for the human TopIB (hTopIB) and the nicking enzyme Nb.BbvCI. hTopIB and Nb.BbvCI represent two extreme cases of strong and mild interaction with DNA during plectoneme release as the former fully encircles the DNA duplex (20) and the latter is expected to release from its substrate after nicking. Plectonemes were released by RepC at a velocity intermediate of that produced by hTopIB and Nb.BbvCI, suggesting a different mode on interaction compared to the other two enzymes. The frequency of religation was also compared between hTopIB and RepC. RepC behaved as an inefficient religating enzyme highlighting its role as a replication initiator instead of as a topoisomerase.

Based on the work described here and structural predictions, we propose a model where RepC nicking activity is force- and twist-dependent. Nicking of DNA at the *dso* by RepC is passive and a consequence of binding to a substrate with the appropriate degree of supercoiling, in which the cruciform structure required for nicking is already present, rather than promoted as a result of RepC binding.

MATERIALS AND METHODS

Proteins

The MBP-RepC fusion protein, in which the maltose binding protein (MBP) is fused to the N- terminal end of RepC, was purified as described earlier (14).

DNA substrates

The pBlueScriptIISK:pT181*cop608* (7217 bp) plasmid was generated by ligating the pBlueScriptIISK+ plasmid (Stratagene) and the pT181*cop608* plasmid (4257 bp) at their KpnI sites (21). The recombinant plasmid was confirmed to be relaxed by RepC by agarose gel analysis (Supplementary Figure S2A). DNA constructs for magnetic

tweezers experiments consisted of a central fragment from the plasmid pBlueScriptIISK:pT181*cop608* flanked with digoxigenin or biotin-labeled DNA handles at its ends (Figure 2A). The central part was constructed from restriction of the plasmid pBlueScriptIISK:pT181*cop608* with *Bam*HI and *Not*I (both from NEB), resulting in a final product of 7194 bp. The handles were PCR-generated from the plasmid pBlueScriptSK+ with appropriate oligos (Supplementary Table S1) adding Dig-dUTP or Bio-dUTP (Roche) in the reaction and followed by restriction with NotI and BamHI, respectively. Subsequent ligation (T4 DNA ligase, NEB) with the central fragment resulted in an 8450 bp product, containing the RepC nicking site at 1480 bp from the biotinylated handle. The ligated product was then used in MT experiments. During the generation of the DNA substrates, we avoided the exposure of the substrates to intercalating agents as well as exposure to UV light. This procedure allowed the isolation of high levels of torsionally-constrained DNA molecules.

The nicking and religation assay of the TopIB enzyme was performed with the same substrate employed in RepC experiments. The nicking assay of nb.BbvCI was performed with a substrate based on the plasmid pSP73-JY0-BbvCI employed in (22) of total length 5358 bp and with a single nicking site at 3106 bp from one end (see Supplementary Methods for more details).

Magnetic-tweezers assays

We employed a custom-built MT setup similar to the system described previously (23,24) with a fast-acquisition camera of maximum frame rate of 500 Hz (Mikrotron MC1362). In our assays, a DNA construct (see above) is tethered between a glass surface covered with anti-digoxigenin and 1-μm streptavidin-coated superparamagnetic beads. A couple of permanent magnets that can be translated along the optical axis of the microscope or rotated are used to twist and stretch the DNA. The bottom surface of the flow cell is considered as zero-height by using reference beads (Ref. Bead) that are attached to the surface and that are not affected by the magnetic field. The magnetic beads are visualized using an inverted optical microscope while the bead position (DNA extension) is measured in real-time by video-microscopy, allowing us to monitor the dynamics of DNA-modifying enzymes at the single-molecule level (22,25). The full system is controlled by an *in-house* LabVIEW software allowing real-time measurements of tens of beads at 60 Hz. More than 1000 DNA molecules were analyzed in this work. The force is calculated from the Brownian excursions of the bead in Fourier space and corrected for low-pass filtering and aliasing (26,27). To determine the spatial resolution of our setup, we followed beads fixed to a glass slide and computed their *xyz* coordinates at 120 Hz. The standard deviations of these histograms for a 20 s window gave values of 2–3 nm for *x* and *y* and 5 nm for the *z* axis.

The integrity of the DNA molecules employed in this study was checked by performing extension versus magnet turns curves at high and low forces. Single torsionally constrained DNA molecules display an asymmetrical response to magnet turns at high force with plectonemes formation only at positive turns, and a symmetrical curve at low forces where plectonemes are formed at both positive and negative turns (Supplementary Figure S2B). From the linear parts of the graph, a change in extension as a function of magnet turns or linking number (ΔLk) could be calculated for a given force. For instance, at 0.34 pN, we obtained a value of 58 nm/turn. These constants allowed us to calculate the rate of supercoil removal, where appropriate.

DNA relaxation measurements were done at the maximum data acquisition velocity of 500 Hz. The rest of experiments were performed at 60 Hz. All the experiments were done at room temperature in a buffer containing 100 mM KCl, 10 mM Tris-HCl, pH 8.0, 10 mM $Mg(CH_3COO)_2$, 10% ethylene glycol, 0.1% Tween-20 and 100 μg/ml BSA. Enzymes were injected into the fluid cell at 18 μl s^{-1}. Typical incubation times were of 2–5 min.

Prediction of the atomic structure of RepC dimer

We have used Phyre2 software to obtain a prediction of the atomic structure for RepC (28). Phyre2 is an online tool that employs an algorithm based on Hidden Markov Models to generate a 3D structure of an input amino acid sequence using as template deposited structures on the PDB. The software returned a structure for the RepC monomer based on RepD (PDB entry 4CWC) having 81% of sequence identity corresponding to the central part of the protein (29). The prediction was obtained with a 100% confidence match. The deposited RepD structure in the PDB is a dimer. In order to obtain a prediction of the dimeric structure for RepC, we aligned two RepC predicted monomers with the respective RepD monomers using PyMOL. Further analysis of the structures and the generation of the figures were carried out with PyMOL Molecular Graphics System (Version 1.8, Schrödinger, LLC).

RESULTS

Nicking and religating activities of RepC protein

The *dso* of the pT181 plasmid consists of 68 bps and includes both a specific RepC-binding sequence and its nicking site (Supplementary Figure S1). The nicking site is within the gap sequence of the inverted repeat element II (IR-II), which is believed to fold to form a cruciform structure. The cruciform structure is not expected to spontaneously form because the IR-II region is GC-rich. However, this energy penalty to form the cruciform could be reduced upon RepC binding (8) or by untwisting the DNA. The nicking and religation reaction of pT181 plasmid with different concentrations of RepC protein in a Mg^{2+}-containing buffer was first analyzed by agarose gel electrophoresis (Supplementary Figure S2A). RepC nicked the supercoiled (SC) plasmid producing relaxed open circular (OC) DNA. RepC also religated the nick as demonstrated by a population of covalently-closed DNA topoisomers distributed around $\Delta Lk = 0$ (TP). This assay confirmed the functional topoisomerase-like activity of RepC as the plasmid was relaxed and religated by the protein.

We developed a MT assay to study the dynamics of RepC nicking and religation activities on individual supercoiled DNA (Figure 2) (30,31). In our assay, a single DNA molecule containing the *dso* that includes both RepC

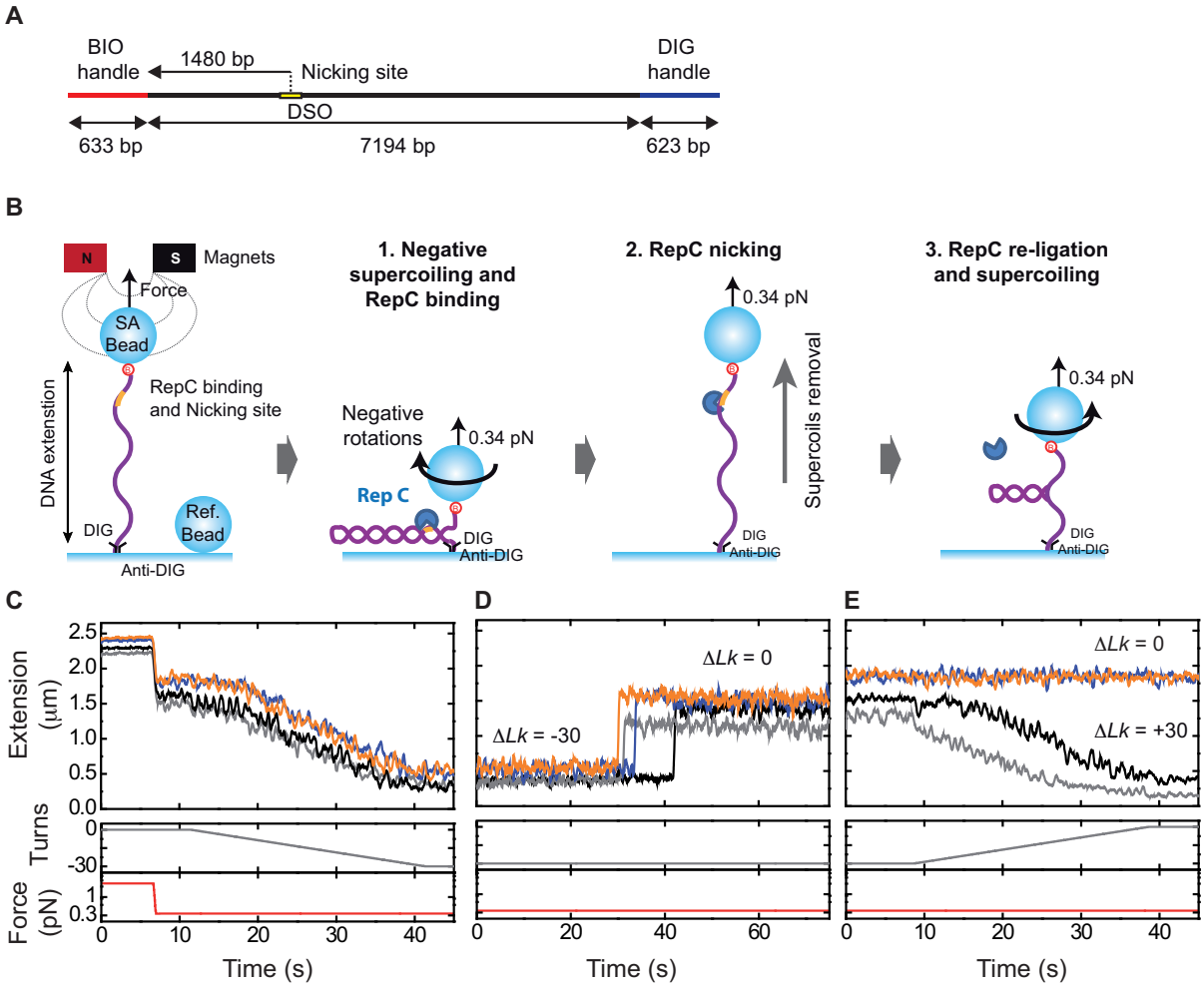

Figure 2. Nicking and religation activities of RepC probed by Magnetic Tweezers (MT). (**A**) DNA substrate employed in MT assays. The substrate contains two handles labeled with biotins and digoxigenins that bind to the magnetic bead and glass surface, respectively. The central part contains the nicking site at 1480 bps from the biotinylated DNA end. (**B**) MT assay. Torsionally-constrained DNA molecules are first negatively supercoiled by applying 30 negative (counter clockwise) rotations (step 1). RepC nicks the DNA and a full recovery of the original height is observed (step 2). To check if DNA molecules can be further coiled, i.e. they have been religated, positive rotations at low force are applied (step 3). (**C**) Extension, Turns and Force time courses that correspond to the supercoiling of torsionally-constrained DNA molecules. (**D**) Nicking activity of RepC. (**E**) RepC religated a fraction of the nicked molecules as they could be further supercoiled by application of positive rotations. Data were acquired at 60 Hz and filtered down to 3 Hz (displayed).

binding and nicking sites is tethered between a streptavidin coated magnetic bead (SA-bead) and the bottom glass surface of a flow cell (Figure 2A). Magnetic beads are manipulated by an external magnetic force produced by a couple of magnets placed above the flow cell. Vertical translation and rotation of the magnets about their axis induces stretching and torsion forces on the DNA molecule, respectively. Our MT assay allows us to supercoil a single torsionally-constrained DNA molecule by rotating the magnets along the optical axis. At low forces, positive or negative supercoils can be produced resulting in a reduction of DNA extension (Supplementary Figure S2B). At high forces, rotation of the magnets in the negative direction induces melting or denaturation of the DNA, while it is still possible to positively supercoil the DNA but with a higher number of magnet rotations (Supplementary Figure S2B). In a typical measurement of RepC activity, a DNA molecule was negatively supercoiled by applying −30 turns (DNA untwisting) at a low force (0.34 pN) causing a decrease of 80% of the original extension (Figure 2B and C). We did not apply a larger number of turns to prevent unspecific binding of the bead to the glass surface. RepC protein was injected into the flow cell with a Mg^{2+}-free buffer. After a few minutes incubation, the volume of the flow cell was exchanged with a Mg^{2+}-containing buffer but without protein. In most cases, we observed a sudden recovery of the initial height of the tethered DNA. This could be interpreted as the result of nicking activity by RepC at the *dso* and the subsequent release of supercoils (Figure 2B and D) and suggests that the protein remained stably bound to the DNA during the buffer exchange process. The relaxation of supercoiled DNA always occurred in a single step. Control experiments performed with RepC in the absence of Mg^{2+} (data not shown) or with molecules lacking the *dso* sequence (Supplementary Figure S3A) did not result in relaxed DNA molecules, thus confirming that the nicking activity observed was in-

deed produced by RepC. Our setup is able to track several single-molecule events simultaneously. For instance, a set of four simultaneously-measured traces are plotted in Figure 2C–E. Interestingly, nicking was not concurrent for all molecules but occurred within the range of a few seconds and this could due to the non-homogeneous arrival of Mg^{2+}. Finally, some DNA molecules could be further supercoiled demonstrating religation activity of RepC in the absence of twist and at an applied force of 0.34 pN (Figure 2E). However, the process of religation was inefficient as most of the DNA molecules remained nicked after several minutes of reaction. This could be due to a potential adverse effect of the rotation of the magnets with the ligation activity or simply to an inherent native low ligation efficiency of RepC.

RepC nicking activity is twist-dependent

The MT experiment described in Figure 2 was repeated with DNA containing positive supercoils. In this case, we did not observe any nicking event as DNA molecules remained supercoiled for several minutes (Supplementary Figure S3B). The inability of RepC to nick positively-supercoiled DNA allowed us to design experiments to probe the mechanistic detail of RepC nicking-religation activities. First, DNA molecules were positively supercoiled by applying +30 turns (anti-clockwise) and then RepC protein was injected into the fluid cell in a Mg^{2+}-containing buffer. Turning the magnets from positive to negative rotations triggered the formation of negative supercoils and nicking by RepC. This is consistent with the protein remaining bound to the DNA during rotation of the magnet, as it was previously suggested in the buffer-exchange experiment (Figure 2). The nicking event can be detected as a sudden change of DNA extension up to its maximum that remains unaltered regardless of the rotation of the magnet (Figure 3A). The rotation of the magnets is coupled to a change in the linking number of the DNA (ΔLk). However, note that because of the presence of magnesium ions in the buffer with RepC, there is an offset of a few positive turns between ΔLk and magnet turns due to the change of supercoiling density of DNA caused by magnesium ions (Figure 3B). The effects on the topology of DNA due to divalent ions are well-characterized (32,33). We therefore took into account these offsets for all the DNA molecules analyzed in this study. Both magnet turns and ΔLk vary equally irrespective of the initial offset produced by the presence of divalent ions, until the moment RepC nicks the DNA and the molecule is relaxed setting ΔLk to zero (Figure 3B). Beyond this point, turning of the magnets had no effect on ΔLk, which remains at zero. These data produced a distribution of ΔLk at the point where RepC nicks the DNA (Figure 3C). The distribution was fitted with a Gaussian function providing a mean value of $\Delta Lk = -9.2 \pm 0.3$ (mean ± s.e.m) and a degree of supercoiling $\sigma = -0.013 \pm 0.004$, calculated as $\Delta Lk \,/\, Lk_0$ where $Lk_0 = n/p$, n is the length of the DNA in nucleotides, and p is the number of base pairs per helical turn (10.5 bp·turn^{-1}). Note that because our experimental procedure consists of progressively applying negative turns, the DNA is more likely to be nicked by RepC before reaching a large negative supercoiling value. The probability of nicking (P) is given by the normalized cumulative integral of the histogram (Figure 3D). This provided a $\Delta Lk_{,\,p:0.5} = -9.5 \pm 0.2$ for a P of 0.5. Since protein activity requires twisting of the DNA, our experiment suggests that RepC nicking is dependent on the formation of a particular structure in the DNA. Moreover, the fact that we only observed protein activity at negative turns, which will favor melting and formation of secondary structures in the DNA, strengthen the idea that a cruciform may be formed.

In order to exclude any effect of concentration in the reported critical linking number required for nicking we repeated the experiment described above for two additional concentrations. Average values of ΔLk were very similar and around −10 (Supplementary Figure S4A and S4B) showing no concentration dependence of RepC nicking activity. We noticed, however, a slightly larger nicking occurrence at larger number of turns for the lower concentration used. We believe this is because of the limited availability of free protein in solution that allowed us to further twist the DNA without observing nicking until a protein binds and nicks the DNA. We also explored if the frequency of twisting of the DNA may influence the probability of nicking occurring at a given force (Supplementary Figure S4C and S4D). Turning the magnets at a lower (0.5 Hz) or higher (1.5 Hz) frequency had a small influence in ΔLk for $P = 0.5$. Efficient nicking occurred always at a value of $\Delta Lk \sim -10$ at the time scale of our experiments (see Supplementary Table S2 for all data statistics).

The dynamic assay reported in Figure 3 has the technical limitation that a minimum number of turns are required to detect a nicking event. The number of turns is coupled to a reduction in extension due to the formation of supercoils (Supplementary Figure S2B). Based on our noise level, sampling rate and measuring force (0.34 pN), we estimate that we minimally need to reduce the extension of the DNA by ∼85 nm prior observing a nicking event, and this is on average four turns (Figure 3A). Below this number of turns it is not possible to distinguish if the molecule has been nicked or not. We therefore performed complementary static experiments where multiple torsionally-constrained DNA molecules were set to a particular degree of twist and exposed to RepC for 1 min. Molecules that were nicked recovered the original extension (Supplementary Figure S5A), in contrast to molecules that remained supercoiled, i.e. not nicked (Supplementary Figure S5B). We also repeated these experiments at zero or near-zero turns. In these cases, we did not observe any reduction of extension, but we could determine if the molecule was nicked after 1 min by simply turning the magnets again. We quantified the fraction of molecules that were nicked after 1 min for different degrees of supercoiling (Supplementary Figure S5C). As expected, none of the molecules were nicked if positively supercoiled, and almost none (2 events out of 40) were nicked at $\Delta Lk = 0$ (torsionally-constrained and relaxed). This measurement contrasts with the nicking rates reported in bulk using quenched-flow experiments and short relaxed linear dsDNA molecules (∼1.5 s^{-1}) (10). Nevertheless, we should also bear in mind that in the previous work the experiments were performed with RepD, a sequence-similar protein and low cross-reactivity has been reported between Rep proteins and the *dso* of different plas-

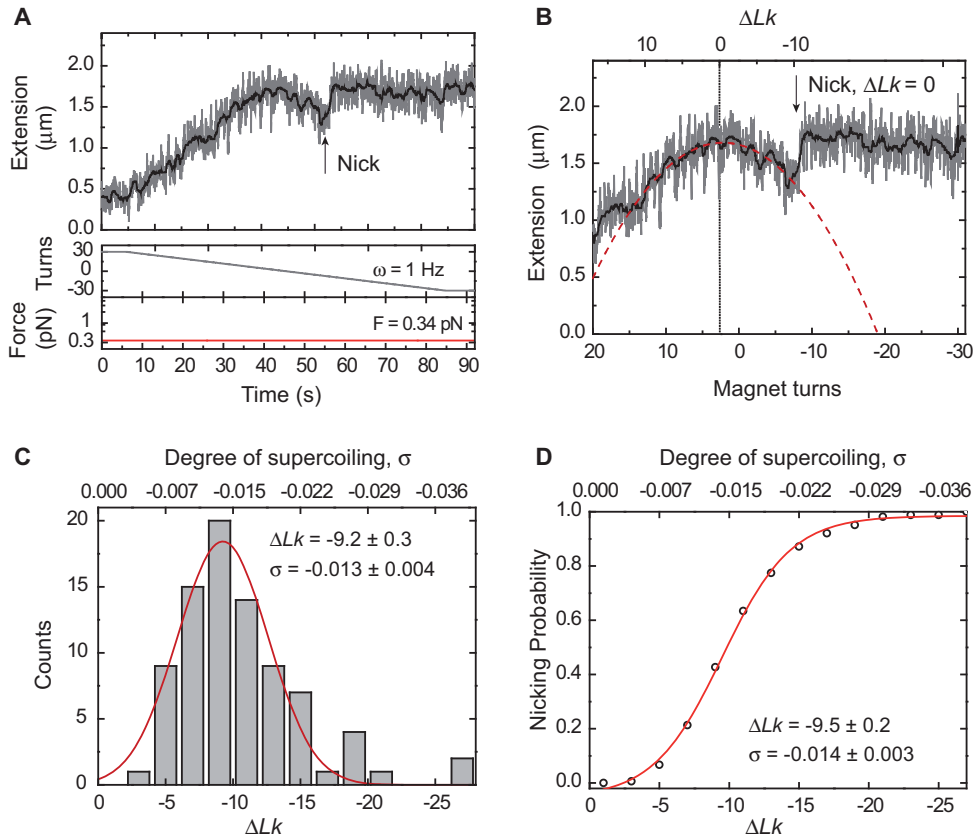

Figure 3. RepC nicking activity occurs only at negative rotations. (**A**) DNA was nicked only at negative turns of the magnet. First, the DNA molecule was positively supercoiled (+30 rotations) and the protein injected in the cell. Then, the molecule was untwisted and negatively supercoiled by applying from +30 to −30 turns. A nick event was detected (see arrow) at −7 turns. (**B**) An offset between magnet turns and linking number was taken into account to determine the ΔLk at which RepC nicked the DNA. Data were acquired at 60 Hz and filtered down to 3 Hz (both displayed). Magnets were rotated at 1 Hz. Force was 0.34 pN, constant in the experiment. (**C**) Histogram of ΔLk (N = 83). The Gaussian fit provides a mean value of ΔLk and supercoiling degree σ (quoted in the figure). (**D**) Normalized cumulative integral of the histogram representing the probability of nicking. Values of ΔLk and σ, quoted in the figure, relate to the characteristic 0.5 probability.

mids (11,34). The fraction of nicked molecules increased as more negative turns were applied following a very similar trend as reported in the continuous rotation experiment (Figure 3).

RepC nicking activity is force-dependent

Our data support the view that a particular topological DNA structure is required for RepC nicking. This nicking was clearly sensitive to twist but it would also be expected to be sensitive to force because the extension-twist behavior of dsDNA is force-dependent (Supplementary Figure S2B). We thus studied the nicking activity of RepC as a function of applied force following the dynamic assay of Figure 3. Because RepC only nicks under a negative turns regime, these experiments were restricted to a range of forces that allowed accumulation of writhe in the DNA (below 1 pN). We did experiments at forces between 0.05 and 1 pN and calculated the probability of nicking as a function of change in linking number. We observed a clear trend where more negative turns must be applied to maintain the probability of nicking, as applied force is reduced (Figure 4A). A linear fit of the data relative to the change in linking number for the characteristic $P = 0.5$ and up to 0.34 pN (Figure 4B, red line) gave a value of about $\sigma = -0.033$ for a negatively-supercoiled plasmid at zero force. An increase of the force up to 0.34 pN implied a 2-fold reduction in supercoiling degree. Beyond this force, we observed leveling of σ values due to the effects arising from melting in the DNA at negative turns at such forces. Melting of the DNA is a pre-requisite to form the cruciform, but if the force is large enough, it will prevent the necessary intrastrand pairing to extrude the cruciform. Indeed, the presence of stable regions of melted DNA has been reported for forces above ∼0.5 pN (23). We also observed that RepC cleavage occurred within a range of turns that became narrower with increasing forces. RepC nicking at forces beyond 1 pN were still possible because we observed that the DNA could not be supercoiled again. However, these nicking events occurred before any reduction in extension, and thus it was not possible to determine the linking number at which RepC nicked the DNA. We expect a progressive reduction of the stability of the cruciform structure for forces above 1 pN until it is definitively inhibited. Opening of hairpins has been reported at forces between 10–14 pN, setting a limit for the formation of secondary structures (35).

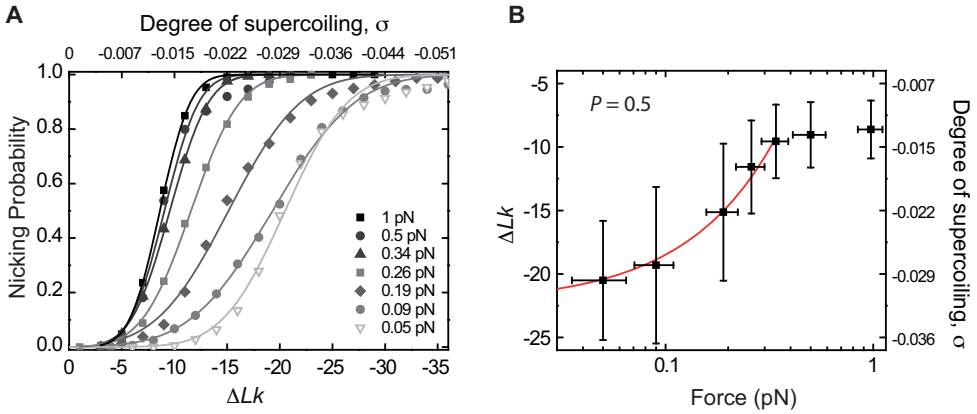

Figure 4. RepC nicking activity is force- and twist-dependent (**A**) Nicking probability as a function of linking number for a range of forces of 0.05–1.0 pN. Probabilities were determined as described in Figure 3. The nicking probability depends on the force applied to the DNA substrate, requiring a larger number of turns at low forces to observe RepC nicking. Also the distributions got sharper at higher forces. (**B**) Characteristic ΔLk ($P = 0.5$) for different forces. The line is a linear fit between 0.05 and 0.34 pN that provides a $\sigma = -0.032$ at zero force.

We next calculated the free energy of supercoiling using the expression $\Delta E = 10 \cdot N \cdot k_B \cdot T \cdot \sigma^2$ (36,37), where N is the number of base pairs, k_B is the Boltzmann constant, and T is the temperature. For $\sigma = -0.033$, we obtained a value of ∼46 kcal/mol. This value is in reasonable agreement with that reported for the formation of cruciform structures involving a small bubble intermediate, namely S-type cruciform structures, which is 40 kcal/mol (38). We also used the model by Marko (39,40–42) to calculate the change of free energy associated to DNA molecules at the supercoiling degree at which we observe nicking, σ_{nick}, for intermediate forces 0.19, 0.26 and 0.34 pN (see Supplementary Material). The results of this analysis were in reasonable agreement with that reported from the extrapolation at zero force and similar to the mentioned energy barrier proposed for a S-type cruciforms.

Our experiments revealed that RepC nicking activity is twist- and force-dependent. The probability of getting a RepC-mediated DNA nicking event increases with applied force for a given number of turns. For instance, a probability of nicking of 0.5 requires −10 turns at 0.35 pN and −20 turns at 0.05 pN. This force dependence on the probability of nicking is consistent with a model where the protein does not apply force on the DNA to form the required DNA structure for nicking. Otherwise, we would have observed a very limited effect of the force on the probability of nicking. Note that even at the very low force of 0.05 pN, the protein could not cleave the DNA unless a considerable number of negative turns were present. This idea contrasts with previously published work that proposed an active role of the protein in extruding the cruciform structure suitable for cleavage (8,9).

RepC–DNA interactions during nicking and religation activities

The accepted mechanism of nicking-closing activity of RepC is that after the introduction of the nick, RepC remains covalently attached to the 5′-end of the nick via a phosphotyrosine bond (11). Measuring the velocity of DNA extension during supercoil release produced by RepC can provide insights into the nature of protein–DNA interactions that take place during nicking events (30). Using a video camera capable of measuring at 500 fps, we were able to resolve in real-time the DNA relaxation curve during supercoil removal by RepC at 0.34 pN, which was characterized by a monotonic increase of DNA extension (Figure 5A). Data were fitted to a linear function to obtain the velocity of plectoneme release in ΔLk per second. The distribution of velocities was fitted to a Gaussian function (Figure 5B) showing a mean value for RepC of around 123 ± 3 ΔLk s^{-1} (mean ± s.e.m.). We performed similar experiments with the human type-IB (hTopIB) topoisomerase (TopoGEN) that nicks the DNA following an identical chemical reaction than RepC, and with the nicking enzyme Nb.BbvCI (New England Biolabs). Experiments with the hTopIB gave a value of 110 ± 2 ΔLk s^{-1} and the nicking enzyme a velocity of 136 ± 5 ΔLk s^{-1}, faster than both RepC and hTopIB.

Our experiments did not reveal large differences in plectoneme release velocities compared to those reported in (30). We explain this discrepancy by the larger force employed in our case that increases the velocity of plectoneme release and may affect the interaction of the DNA with the protein. Still, our data consistently indicated an intermediate behavior of RepC between the fastest response produced by the nicking enzyme and the slowest behavior shown by the topoisomerase. We believe these differences in plectoneme release velocities reflect different types of protein–DNA interactions.

These differences between hTopIB and RepC became more evident in subsequent nicking-religation experiments (Figure 5C–F). As mentioned above, RepC could only nick negatively supercoiled DNA containing the *dso* sequence (Figure 5C and D). Once nicked, we continuously rotated the magnet in the negative direction with the aim of negatively supercoiling the DNA again. If the protein seals the nick, we should expect to see a decrease in extension at the force employed in the assay (0.34 pN). RepC behaved as a very inefficient religating enzyme. Cycles of nicking and religation over the same molecule were rarely observed and

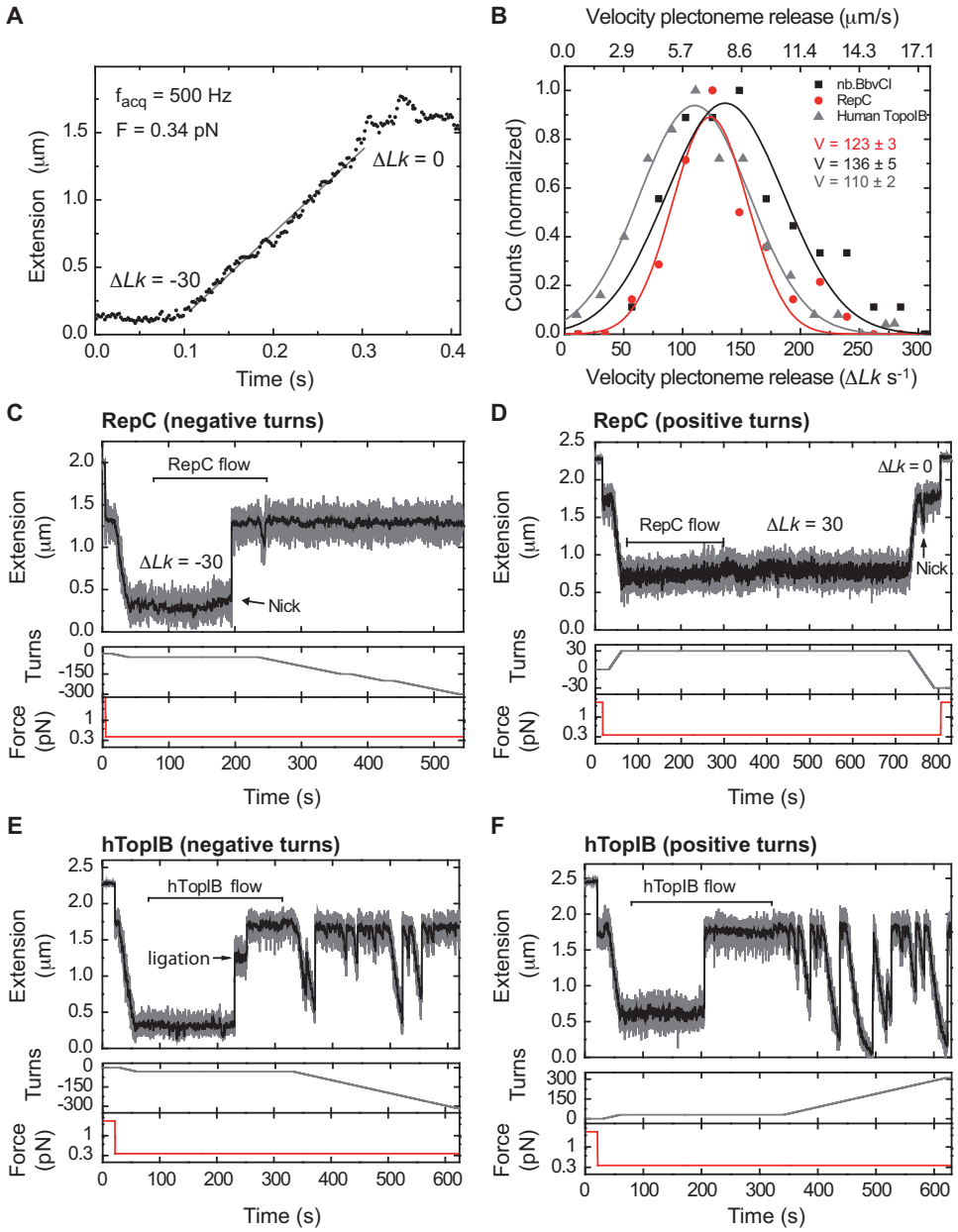

Figure 5. RepC–DNA interaction during nicking and religation activities. (**A**) Characteristic supercoils removal time course taken at 0.34 pN. Approximately 30 turns were released in 0.3 s. Data were acquired at 500 Hz. (**B**) Histogram of velocities of plectoneme release for RepC, hTopIB and Nb.BbvCI. Frequencies are fitted to a Gaussian function and the mean and s.e.m values are quoted in the figure. RepC showed an intermediate velocity between the topoisomerase and the nicking enzyme. (**C**) Nicking and religation experiment with RepC. RepC occasionally religated the nicked DNA. This is shown as a dip in the extension while the magnets continuously rotate in a negative direction. (**D**) RepC cannot nick positively supercoiled DNA. (**E** and **F**) Nicking and religation experiment with hTopIB. hTopIB nicks and religates efficiently while the magnets continuously rotate in either negative or positive direction.

very often the molecule was never religated back or required a long time for religation. In the example shown in Figure 5C, RepC religated the DNA just once in about 6 min while it remained covalently linked to the DNA. However, other experiments did not show religation activity of RepC for tens of minutes. Long religation times for RepC has been described before in bulk biochemical assays (10). DNA supercoils were released by RepC protein always in a single step and this is consistent with the very low religating rate of the enzyme. In contrast, hTopIB could nick both positively and negatively supercoiled DNA and religate nicks very efficiently (2.5 s^{-1}) for multiple cycles during the course of the experiment (Figure 5E and F). Occasionally, we observed a multistep relaxation curve as it has been previously reported (see arrow in Figure 5E) (30). Differences in religation activities of hTopIB and RepC reveal a very different interaction with the DNA, and it likely reflects their different specialized functions in the cell.

The poor religating activity of RepC was further confirmed in the assay performed in the absence of continuous

magnet rotations (Supplementary Figure S5C). The example shown in Supplementary Figure S5D is a positive religation case, but this was uncommon as only about 11% of the molecules were religated after 1 min incubation at $\Delta Lk = -8$ turns and -4 turns. The weak religation activity of RepC is consistent with its role in pT181 replication since after nicking it is not expected to religate the DNA immediately. Instead, after RepC-mediated nicking, plasmid replication is initiated, and only after the leading strand has been synthesized, RepC is expected to religate the DNA after cleaving the DNA at the regenerated nick site (see Figure 1). Since there is no DNA replication in our experiments, it makes sense that RepC is able to religate the nicked DNA substrates at a very low efficiency.

DISCUSSION

This work reports the first use of MT to directly measure RepC nicking at the single-molecule level. The advantage of MT over other single-molecule approaches is that a controlled force and/or twist can be applied to a single DNA molecule. Thus, information related to the degree of DNA supercoiling required for a specific enzymatic reaction can be obtained. In our assays, the extension of a dsDNA molecule is followed in real-time and changes arising from the nicking of a supercoiled substrate can be detected with millisecond and nanometer resolution. Here, we show that the nicking activity of RepC is force- and twist-dependent suggesting that it requires particular torsional conditions for its specific activity. We argue below that it is not the torque the critical parameter for RepC nicking, but a certain supercoiling energy, which grows linearly with the number of turns. We also highlight a particular mode of interaction of RepC with the DNA which is different from that of the topoisomerase hTopIB that cleaves DNA using the same chemical mechanism.

Rep proteins were observed to nick and religate negatively supercoiled plasmid DNA containing the *dso in vitro* to form relaxed, covalently-closed molecules (5). This is consistent with the idea that formation of the nicking site for RepC is favored by the presence of negative supercoils, as reported in this study. However, nicking activity for RepD, an homologous protein performing replication initiation in the *staphylococcal* plasmid pC221, has been observed to nick linear dsDNA substrates containing the *dso* although with a much lower nicking rate constant than for supercoiled plasmids (10,11,43). In our assay, we never observed nicking of positively supercoiled DNA and very rarely nicking of relaxed torsionally constrained DNA subjected to a force as low as 0.34 pN.

Previous work has shown that the presence of a cruciform structure increases the efficiency of replication initiation (9). However, it is not fully understood if the cruciform structure is spontaneously formed under certain conditions of force and twist and RepC just binds and nicks the substrate, or if the Rep protein actively promotes formation of this structure upon binding and then nicks the substrate. Spontaneous formation of cruciform structures has been detected using MT as sudden changes in the extension of the DNA of hundreds of nanometers (44). However, we were unable to detect any change of extension attributable to the formation of the cruciform structure using similar forces, supercoiling and working conditions in our setup (not shown). This is very likely due to the different nucleotide sequence of the DNA substrate used in our study, as similar changes in extension as reported in (44) could be easily detected with our setup. Spontaneous formation of the cruciform structure at zero twist is very unlikely because the nick site of RepC in the pT181 DNA is at the tip of an inverted repeat element with much higher GC content than the rest of the plasmid. Consequently, it has been proposed that it is the binding of RepC that melts this region resulting in the extrusion of the inverted repeat element forming the cruciform structure needed for cleavage (9,45). However, we did not observe any change in extension that could be interpreted as the extrusion of the cruciform by RepC binding in a Mg^{2+}-free buffer (Supplementary Figure S6). Instead, our data are consistent with a passive model (see below), where RepC binds at the *dso* but does not induce formation of the cruciform. Firstly, we found that at 0.34 pN RepC cleaves the DNA at a degree of supercoiling corresponding to $\sim\Delta Lk = -10$, and that was largely insensitive to the speed of twisting of the DNA. This supports the idea that the structure suitable for cleavage is formed at a particular supercoiling degree. Secondly, we found that the probability of nicking is force-dependent. An active extrusion of the cruciform by the protein would have made RepC nicking activity largely insensitive to the range of the very low forces (0.05–1 pN) employed here, contrary to what we observed. Rather, RepC nicking activity was affected by the force and by the twist applied to the substrate. Our observation is that as the stretching force on the DNA is reduced, a larger number of negative turns are required to detect RepC nicking (Figure 4).

We report here the first precise measurement of the degree of DNA supercoiling necessary for DNA relaxation by Rep proteins. We determined a value of $\sigma = -0.032$ in the absence of force. Previous studies have made efforts to measure the degree of DNA supercoiling *in vivo*. It has been proposed that for *E. coli*, the average degree of supercoiling is $\sigma \approx -0.05$ (46). In contrast, Bliska and Cozzarelli (47) showed that in *E. coli* the effective, purely torsional degree of supercoiling in the absence of protein stabilization was -0.025. Our measurement is therefore similar to the supercoiling degree found *in vivo*. This supports a model in which the cruciform structure forms passively due to the natural supercoiling of DNA, with RepC making only a minor contribution to its formation.

It has been proposed that the crossover where two DNA helices juxtapose can be a recognizable structure for supercoiling-sensitive proteins (48). We have discarded this possibility because at low forces plectonemes are formed with a lower number of turns and consequently nicking would occur earlier than at high forces, contrary to our observation. RepC nicking occurs in the plectonemic regime where the torque is constant, regardless of the number of turns. If a particular torque was required for RepC nicking, at very low forces we should not have observed nicking because that torque could not have been reached. Therefore, it is not the torque the critical parameter for RepC nicking. Instead, we propose that the structure formed on the DNA needed for RepC nicking requires a characteristic supercoiling energy for its formation, because in the plec-

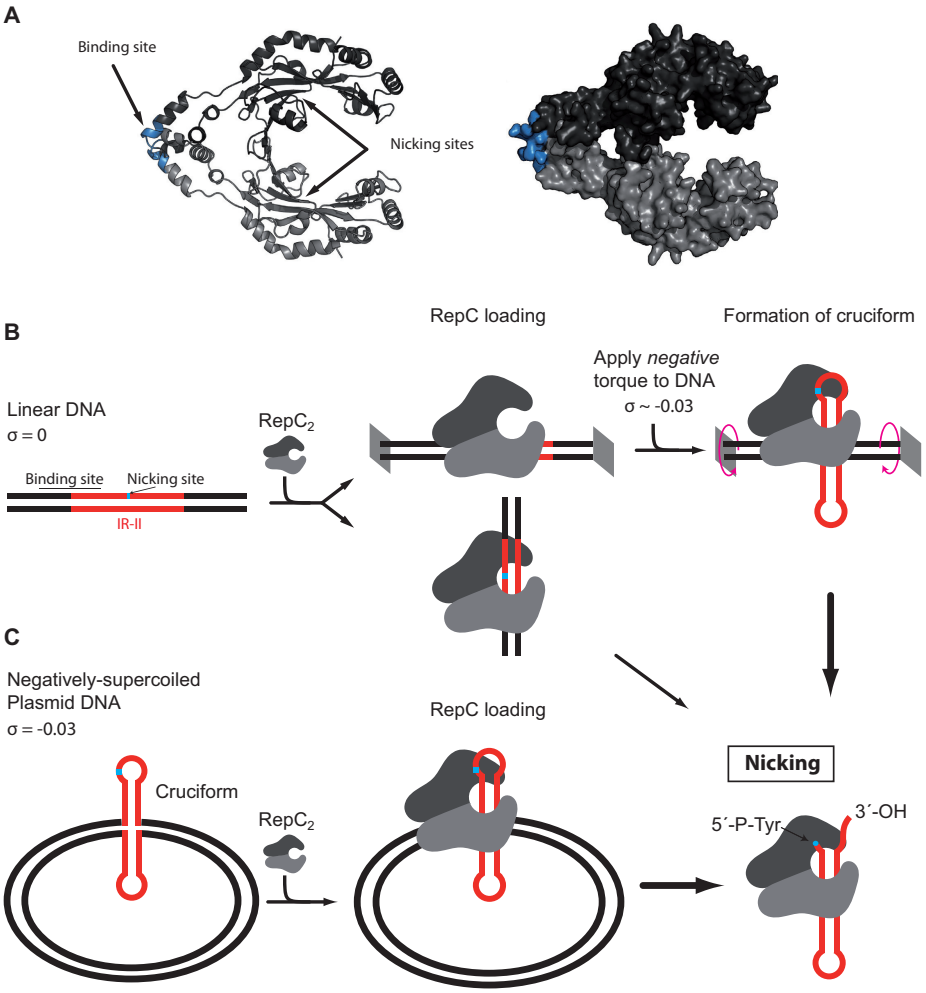

Figure 6. Passive nicking model for RepC. (**A**) Phyre2 prediction of the structure of RepC based on its 80% sequence homology with RepD (PDB entry 4CWC). RepC is a dimer with separate DNA binding (blue) and nicking domains (arrows). It has a C-shape morphology with a cavity of 30-40 Å, enough to accommodate the DNA for cleavage. (**B**) RepC binds to linear DNA but does not nick it because the cruciform structure is not induced. Application of a twist in a torsionally-constrained linear DNA produces extrusion of the cruciform and places the tip of the hairpin at the catalytic site of RepC resulting in efficient nicking. Nicking of linear DNA is inefficient as it would require sliding of the molecule through the cavity of RepC or direct binding to the nicking site. (**C**) A negatively supercoiled plasmid already contains the appropriate cruciform structure and is a substrate for RepC binding and efficient nicking.

tonemic regime it is the energy which grows linearly with the number of turns. We estimated a free energy associated with the degree of supercoiling required for nicking of 45 kcal/mol. This value is similar to the reported activation energies of S-type cruciform extrusion (38). S-type cruciforms are much more common than the C-type cruciform in which extrusion is dependent on a higher energy barrier (180–200 kcal/mol) (38,49). The fact that the energy applied to the DNA to observe a nick by RepC coincides with the value reported for the extrusion of S-type cruciforms, further supports a passive model for RepC nicking activity. Once the critical degree of supercoiling is reached, the mechanism by which the protein recognizes the resulting secondary structure is not clear, and has been the subject of various studies (8,9,18).

We have used the Phyre2 software to predict the structure for RepC (28). We found a very high confidence result based on the available structure of the closely-related RepD dimer (PDB entry 4CWC) (29). The predicted structure is symmetric, despite RepC nicks only negative turns. This is not uncommon, as other chiral homodimer proteins have shown preference for cruciform structures or positively supercoiled DNA (50,51). RepC formed a C-shape dimer structure with a cavity of ∼30–40 Å internal diameter, where the catalytic tyrosine-191 responsible for DNA nicking is located. The C-shape predicted structure is compatible with the presence of friction that slows down the velocity of supercoil release and this is consistent with our measurements. Interestingly, residues 265–270 of RepC involved in its DNA binding activity (52) are located outside the cavity, on the convex side (Figure 6A). Based on this structure and the experimental evidence reported here, we propose a model for RepC binding and nicking where both activities are independent. In linear torsionally-constrained DNA substrates RepC first binds and only when appropriate torque conditions are applied to the DNA, the cruciform forms, facilitating the con-

tact of the nicking site with catalytic site of RepC (Figure 6B, upper path). End-free DNA may also be cleaved but that would require the sliding of one of the free ends of the DNA through the cavity where the catalytic site is located (Figure 6B, lower path). In negatively-supercoiled DNA, the cruciform structure can be preformed, and binding of RepC facilitates nicking because the nicking site is immediately placed in the active site of the RepC dimer (Figure 6C). This passive nicking model of RepC is compatible with previous observations that RepC can nick both linear dsDNA and ssDNA (53,54) as well as other dsDNA structures with free ends (10). Linear substrates may just occasionally make contact with the active site resulting in cleavage. This should in principle result in much lower nicking rates than those found for plasmids as has been reported (10), and supports the idea that nicking is favored by supercoiling. Indeed, plasmid DNA replication is initiated only when the DNA is supercoiled (55).

Supercoil-release experiments and nicking-religation assays with RepC and hTopIB revealed different interaction modes of these enzymes with the DNA, despite the fact that both nick and religate the DNA through the same chemical reaction. hTopIB could nick both positively and negatively supercoiled substrates and seal the nick with high efficiency (30,56). In contrast, RepC could only nick negatively supercoiled DNA and had very poor religation efficiency. These differences are likely a consequence of their distinct functions in the cell and we believe the cruciform structure is key to understanding their own mechanisms of functioning. In fact, because cruciform formation requires DNA melting, it will only form at negative turns, and this sets an additional filter for the selection of the replication initiator, increasing protein–DNA specificity. What happens with the cruciform structure when the DNA is nicked remains an open question, and the answer may explain why the religation activity is so low. Disruption of the cruciform by nicking may impede the correct placement of the 3′OH of the DNA at the catalytic domain of the Rep protein to seal the nick. The low efficiency of religation could be beneficial for the function of the enzyme that needs to load PcrA helicase to begin DNA unwinding during the process of RCR. A very fast religation rate would certainly hinder the helicase loading and replication initiation, as well as increase DNA–RepC protein exchange. Understanding at the single-molecule level how PcrA is loaded onto the DNA after RepC nicking and how this and the unwinding activities are affected by force and twist will be the subject of future work.

Our MT assay provides a basis to recapitulate at the single-molecule and in real-time the process of rolling-circle replication. Magnetic Tweezers allowed us to mimic the supercoiled state of plasmids and to investigate how this affects nicking and religation activities of replication initiator proteins involved in the first step of RCR. Our work highlights the relevance of the formation of the cruciform structure for RepC nicking, whose activity was dependent on the force and the twist applied to the DNA. We propose a passive model where RepC cleaves the appropriate structure when it is formed at a particular supercoiling energy imposed by force and twist. The implications of these mechanical requirements for nicking likely explain the low religation efficiency of this enzyme and provide a possible explanation for the differences observed with other nicking-religating enzymes such as type IB topoisomerases.

SUPPLEMENTARY DATA

Supplementary Data are available at NAR Online.

ACKNOWLEDGEMENTS

The authors are grateful to Gemma Fisher, Adriana Gil and Mark S. Dillingham for their comments on the manuscript; and to Alberto Marín for helpful discussions. C.C. acknowledges support from the Spanish Ministry of Science through a Juan de la Cierva contract ref JCI-2011-10277.
Author contributions: C.L.P. and C.C. performed the magnetic tweezers experiments and construction of the DNA substrates. P.A. generated the recombinant plasmids and purified the proteins. F.M.H. wrote the manuscript. C.L.P., C.C. and F.M.H. designed the experiments. All authors were involved in the data interpretation and revising of the manuscript.

FUNDING

Spanish Ministry of Economy and Competitiveness [FIS2014-58328-P and FIS2014-51481-ERC to F.M.H.]; NIH [GM31685 to S.A.K. and GM068406 to S.H.L.]. Funding for open access charge: Spanish Ministry of Economy and Competitiveness [FIS2014-58328-P to F.M.H.].
Conflict of interest statement. None declared.

REFERENCES

1. del Solar,G., Giraldo,R., Ruiz-Echevarria,M.J., Espinosa,M. and Diaz-Orejas,R. (1998) Replication and control of circular bacterial plasmids. *Microbiol. Mol. Biol. Rev.*, **62**, 434–464.
2. Khan,S.A. (1997) Rolling-circle replication of bacterial plasmids. *Microbiol. Mol. Biol. Rev.*, **61**, 442–455.
3. Ruiz-Maso,J.A., Macho,N.C., Bordanaba-Ruiseco,L., Espinosa,M., Coll,M. and Del Solar,G. (2015) Plasmid rolling-circle replication. *Microbiol. Spectr.*, **3**, 1–23.
4. Khan,S.A. (1996) Mechanism of replication and copy number control of plasmids in gram-positive bacteria. *Genet. Eng. (N.Y.)*, **18**, 183–201.
5. Koepsel,R.R., Murray,R.W., Rosenblum,W.D. and Khan,S.A. (1985) The replication initiator protein of plasmid pT181 has sequence-specific endonuclease and topoisomerase-like activities. *Proc. Natl. Acad. Sci. U.S.A.*, **82**, 6845–6849.
6. Khan,S.A. (2005) Plasmid rolling-circle replication: highlights of two decades of research. *Plasmid*, **53**, 126–136.
7. Koepsel,R.R., Murray,R.W., Rosenblum,W.D. and Khan,S.A. (1985) Purification of pT181-encoded repC protein required for the initiation of plasmid replication. *J. Biol. Chem.*, **260**, 8571–8577.
8. Jin,R., Fernandez-Beros,M.E. and Novick,R.P. (1997) Why is the initiation nick site of an AT-rich rolling circle plasmid at the tip of a GC-rich cruciform? *EMBO J.*, **16**, 4456–4466.
9. Noirot,P., Bargonetti,J. and Novick,R.P. (1990) Initiation of rolling-circle replication in pT181 plasmid: initiator protein enhances cruciform extrusion at the origin. *Proc. Natl. Acad. Sci. U.S.A.*, **87**, 8560–8564.
10. Arbore,C., Lewis,L.M. and Webb,M.R. (2012) Kinetic mechanism of initiation by RepD as a part of asymmetric, rolling circle plasmid unwinding. *Biochemistry*, **51**, 3684–3693.
11. Thomas,C.D., Balson,D.F. and Shaw,W.V. (1990) In vitro studies of the initiation of staphylococcal plasmid replication. Specificity of RepD for its origin (oriD) and characterization of the Rep-ori tyrosyl ester intermediate. *J. Biol. Chem.*, **265**, 5519–5530.

12. Zhang,W., Dillingham,M.S., Thomas,C.D., Allen,S., Roberts,C.J. and Soultanas,P. (2007) Directional loading and stimulation of PcrA helicase by the replication initiator protein RepD. *J. Mol. Biol.*, **371**, 336–348.
13. Gutierrez,C., Martin,G., Sogo,J.M. and Salas,M. (1991) Mechanism of stimulation of DNA replication by bacteriophage phi 29 single-stranded DNA-binding protein p5. *J. Biol. Chem.*, **266**, 2104–2111.
14. Chang,T.L., Kramer,M.G., Ansari,R.A. and Khan,S.A. (2000) Role of individual monomers of a dimeric initiator protein in the initiation and termination of plasmid rolling circle replication. *J. Biol. Chem.*, **275**, 13529–13534.
15. Rasooly,A. and Novick,R.P. (1993) Replication-specific inactivation of the pT181 plasmid initiator protein. *Science*, **262**, 1048–1050.
16. Gruss,A.D., Ross,H.F. and Novick,R.P. (1987) Functional analysis of a palindromic sequence required for normal replication of several staphylococcal plasmids. *Proc. Natl. Acad. Sci. U.S.A.*, **84**, 2165–2169.
17. Kramer,M.G., Khan,S.A. and Espinosa,M. (1997) Plasmid rolling circle replication: identification of the RNA polymerase-directed primer RNA and requirement for DNA polymerase I for lagging strand synthesis. *EMBO J.*, **16**, 5784–5795.
18. Gennaro,M.L., Iordanescu,S., Novick,R.P., Murray,R.W., Steck,T.R. and Khan,S.A. (1989) Functional organization of the plasmid pT181 replication origin. *J. Mol. Biol.*, **205**, 355–362.
19. Koepsel,R.R. and Khan,S.A. (1986) Static and initiator protein-enhanced bending of DNA at a replication origin. *Science*, **233**, 1316–1318.
20. Redinbo,M.R., Stewart,L., Kuhn,P., Champoux,J.J. and Hol,W.G. (1998) Crystal structures of human topoisomerase I in covalent and noncovalent complexes with DNA. *Science*, **279**, 1504–1513.
21. Khan,S.A. and Novick,R.P. (1983) Complete nucleotide sequence of pT181, a tetracycline-resistance plasmid from Staphylococcus aureus. *Plasmid*, **10**, 251–259.
22. Carrasco,C., Gilhooly,N.S., Dillingham,M.S. and Moreno-Herrero,F. (2013) On the mechanism of recombination hotspot scanning during double-stranded DNA break resection. *Proc. Natl. Acad. Sci. U.S.A.*, **110**, E2562–E2571.
23. Strick,T.R., Allemand,J.F., Bensimon,D. and Croquette,V. (1998) Behavior of supercoiled DNA. *Biophys. J.*, **74**, 2016–2028.
24. Seidel,R., van Noort,J., van der Scheer,C., Bloom,J.G., Dekker,N.H., Dutta,C.F., Blundell,A., Robinson,T., Firman,K. and Dekker,C. (2004) Real-time observation of DNA translocation by the type I restriction modification enzyme EcoR124I. *Nat. Struct. Mol. Biol.*, **11**, 838–843.
25. Taylor,J.A., Pastrana,C.L., Butterer,A., Pernstich,C., Gwynn,E.J., Sobott,F., Moreno-Herrero,F. and Dillingham,M.S. (2015) Specific and non-specific interactions of ParB with DNA: implications for chromosome segregation. *Nucleic Acids Res.*, **43**, 719–731.
26. te Velthuis,A.J., Kerssemakers,J.W., Lipfert,J. and Dekker,N.H. (2010) Quantitative guidelines for force calibration through spectral analysis of magnetic tweezers data. *Biophys. J.*, **99**, 1292–1302.
27. Daldrop,P., Brutzer,H., Huhle,A., Kauert,D.J. and Seidel,R. (2015) Extending the range for force calibration in magnetic tweezers. *Biophys. J.*, **108**, 2550–2561.
28. Kelley,L.A., Mezulis,S., Yates,C.M., Wass,M.N. and Sternberg,M.J. (2015) The Phyre2 web portal for protein modeling, prediction and analysis. *Nat. Protoc.*, **10**, 845–858.
29. Carr,S.B., Phillips,S.E. and Thomas,C.D. (2016) Structures of replication initiation proteins from staphylococcal antibiotic resistance plasmids reveal protein asymmetry and flexibility are necessary for replication. *Nucleic Acids Res.*, **44**, 2417–2428.
30. Koster,D.A., Croquette,V., Dekker,C., Shuman,S. and Dekker,N.H. (2005) Friction and torque govern the relaxation of DNA supercoils by eukaryotic topoisomerase IB. *Nature*, **434**, 671–674.
31. Strick,T.R., Allemand,J.F., Bensimon,D., Bensimon,A. and Croquette,V. (1996) The elasticity of a single supercoiled DNA molecule. *Science*, **271**, 1835–1837.
32. Xu,Y.C. and Bremer,H. (1997) Winding of the DNA helix by divalent metal ions. *Nucleic Acids Res.*, **25**, 4067–4071.
33. Rybenkov,V.V., Vologodskii,A.V. and Cozzarelli,N.R. (1997) The effect of ionic conditions on DNA helical repeat, effective diameter and free energy of supercoiling. *Nucleic Acids Res.*, **25**, 1412–1418.
34. Iordanescu,S. (1989) Specificity of the interactions between the Rep proteins and the origins of replication of Staphylococcus aureus plasmids pT181 and pC221. *Mol. Gen. Genet.*, **217**, 481–487.
35. Essevaz-Roulet,B., Bockelmann,U. and Heslot,F. (1997) Mechanical separation of the complementary strands of DNA. *Proc. Natl. Acad. Sci. U.S.A.*, **94**, 11935–11940.
36. Vologodskii,A.V., Lukashin,A.V., Anshelevich,V.V. and Frank-Kamenetskii,M.D. (1979) Fluctuations in superhelical DNA. *Nucleic Acids Res.*, **6**, 967–982.
37. Pulleyblank,D.E., Shure,M., Tang,D., Vinograd,J. and Vosberg,H.P. (1975) Action of nicking-closing enzyme on supercoiled and nonsupercoiled closed circular DNA: formation of a Boltzmann distribution of topological isomers. *Proc. Natl. Acad. Sci. U.S.A.*, **72**, 4280–4284.
38. Lilley,D.M.J. (1989) Structural isomerization in DNA: The formation of cruciform structures in supercoiled DNA molecules. *Chem. Soc. Rev.*, **18**, 53–83.
39. Marko,J.F. (2007) Torque and dynamics of linking number relaxation in stretched supercoiled DNA. *Phys. Rev. E Stat. Nonlin. Soft Matter Phys.*, **76**, 021926–021939.
40. Lipfert,J., Kerssemakers,J.W., Jager,T. and Dekker,N.H. (2010) Magnetic torque tweezers: measuring torsional stiffness in DNA and RecA-DNA filaments. *Nat. Methods*, **7**, 977–980.
41. Lipfert,J., Wiggin,M., Kerssemakers,J.W., Pedaci,F. and Dekker,N.H. (2011) Freely orbiting magnetic tweezers to directly monitor changes in the twist of nucleic acids. *Nat. Commun.*, **2**, 439.
42. Moroz,J.D. and Nelson,P. (1997) Torsional directed walks, entropic elasticity, and DNA twist stiffness. *Proc. Natl. Acad. Sci. U.S.A.*, **94**, 14418–14422.
43. Chisty,L.T., Toseland,C.P., Fili,N., Mashanov,G.I., Dillingham,M.S., Molloy,J.E. and Webb,M.R. (2013) Monomeric PcrA helicase processively unwinds plasmid lengths of DNA in the presence of the initiator protein RepD. *Nucleic Acids Res.*, **41**, 5010–5023.
44. Ramreddy,T., Sachidanandam,R. and Strick,T.R. (2011) Real-time detection of cruciform extrusion by single-molecule DNA nanomanipulation. *Nucleic Acids Res.*, **39**, 4275–4283.
45. Jin,R. and Novick,R.P. (2001) Role of the double-strand origin cruciform in pT181 replication. *Plasmid*, **46**, 95–105.
46. Wang,J.C. (1984) DNA supercoiling and its effects on the structure of DNA. *J. Cell Sci. Suppl.*, **1**, 21–29.
47. Bliska,J.B. and Cozzarelli,N.R. (1987) Use of site-specific recombination as a probe of DNA structure and metabolism in vivo. *J. Mol. Biol.*, **194**, 205–218.
48. Zechiedrich,E.L. and Osheroff,N. (1990) Eukaryotic topoisomerases recognize nucleic acid topology by preferentially interacting with DNA crossovers. *EMBO J.*, **9**, 4555–4562.
49. Bikard,D., Loot,C., Baharoglu,Z. and Mazel,D. (2010) Folded DNA in action: hairpin formation and biological functions in prokaryotes. *Microbiol. Mol. Biol. Rev.*, **74**, 570–588.
50. Crisona,N.J., Strick,T.R., Bensimon,D., Croquette,V. and Cozzarelli,N.R. (2000) Preferential relaxation of positively supercoiled DNA by E. coli topoisomerase IV in single-molecule and ensemble measurements. *Genes Dev.*, **14**, 2881–2892.
51. Zannis-Hadjopoulos,M., Yahyaoui,W. and Callejo,M. (2008) 14-3-3 cruciform-binding proteins as regulators of eukaryotic DNA replication. *Trends Biochem. Sci.*, **33**, 44–50.
52. Dempsey,L.A., Birch,P. and Khan,S.A. (1992) Six amino acids determine the sequence-specific DNA binding and replication specificity of the initiator proteins of the pT181 family. *J. Biol. Chem.*, **267**, 24538–24543.
53. Koepsel,R.R. and Khan,S.A. (1987) Cleavage of single-stranded DNA by plasmid pT181-encoded RepC protein. *Nucleic Acids Res.*, **15**, 4085–4097.
54. Koepsel,R.R., Murray,R.W. and Khan,S.A. (1986) Sequence-specific interaction between the replication initiator protein of plasmid pT181 and its origin of replication. *Proc. Natl. Acad. Sci. U.S.A.*, **83**, 5484–5488.
55. Khan,S.A., Carleton,S.M. and Novick,R.P. (1981) Replication of plasmid pT181 DNA in vitro: requirement for a plasmid-encoded product. *Proc. Natl. Acad. Sci. U.S.A.*, **78**, 4902–4906.
56. Champoux,J.J. (2001) DNA topoisomerases: structure, function, and mechanism. *Annu. Rev. Biochem.*, **70**, 369–413.